The Role of Chemically Modified DNA in Discrimination of Single Point Mutation through Plasmon-based Colorimetric Assays

María Sanromán-Iglesias[†], Charles H. Lawrie[‡,ǁ], Luis M. Liz-Marzán[†,ǁ,§], Marek Grzelczak[†,ǁ*]

[†]CIC biomaGUNE, Paseo de Miramón 182, 20014 Donostia-San Sebastián, Spain

[‡] Oncology Area, Biodonostia Research Institute, Paseo Doctor Begiristain, s/n, 20014, Donostia-San Sebastián, Spain

[ǁ]Ikerbasque, Basque Foundation for Science, 48013 Bilbao, Spain

[§] CIBER de Bioingeniería, Biomateriales y Nanomedicina, CIBER-BBN, 20014 Donostia-San Sebastián, Spain

[§]Donostia International Physics Center, Paseo de Manuel Lardizabal 4, 20018Donostia-San Sebastián, Spain

KEYWORDS: DNA modifications, single nucleotide polymorphism, colorimetric assay, gold nanoparticles, EGFR biomarker

ABSTRACT: The use of gold nanoparticles for the colorimetric detection of single nucleotide mutations associated with cancer in liquid biopsies is a promising strategy for early cancer diagnosis. In order to realize this technology, the sensor must discriminate mutations in double stranded (ds)DNA with an average length of ~140 bp. Here we compared ssDNA and dsDNA of differing lengths (70 and 140 bp) and the effect of chemical modifications (2'-OMe vs. 2'-F) on the DNA probe sequence stabilizing gold nanoparticles of either 25 or 50 nm. We confirmed that the performance of the single nucleotide polymorphism (SNP) detection decreases with both the increase of the length of the sequences and the incorporation of dsDNA architecture. We found that for the larger particles the sensitivity of assay increases, while selectivity of the assay is better for smaller particles. Finally, the presence of 2'-F modification improves detection of SNP in ssDNA while 2'-OMe modification is better for SNP detection in dsDNA.

Monitoring disease in a non-invasive manner through the detection of biomarkers in biological fluids such as blood (*i.e.* liquid biopsies) has the potential to revolutionize the management of cancer patients.[1] Of particular note is the detection of single nucleotide mutations in genes including *BRAF, KRAS* or *EGFR* that result in a patient receiving specific targeted treatment.[2–6] The main challenge for colorimetric discrimination of SNP is the length of sequences that on average is ~140 base pairs, and that double-stranded DNA (dsDNA) can hinder the accessibility of the mutated base during the detection process.[9] The detection of SNP in long single-stranded DNA (ssDNA) can be equally challenging because of the possible secondary structure formation.[10] Therefore, the length of analyte DNA and the eventual inaccessibility of the mutated base require proper biosensing design. In colloid-based sensing, such a design translates into either the size/shape of the nanoparticles or the chemical structure of DNA anchored onto the nanoparticle surface (capture probes).

Polymer Chain Reaction,[11–14] a technique enabling fast screening of mutations in dsDNA, serves as a conceptual framework for the development of assays relying on its principle, *i.e.*, thermal annealing of dsDNA, splitting complementary strands, and discrimination of mutated sequences through a given signal transduction method. Particularly attractive is the use of blocking probes, which prevent reassociation of denatured DNA strands after thermal annealing, allowing the detection of mutated dsDNA with no need for enzymatic amplification. In fact, the blocking strategy has been proposed for SNP detection in dsDNA using an electrochemical assay.[15,16] Similarly, successful implementation of the blocking strategy has been reported in colloidal biosensors.[17–21] However, regardless the transduction mechanism – electrochemistry or colloidal events - dsDNA blocking requires a pretreatment step to expose the mutated bases for a given capture probe. Thus, further effort is required to devise a system in which the dsDNA blocking and SNP detection take place in a single process.

Chemical modification of nucleic acids has been shown to improve their stability against nucleolytic and enzymatic degradation.[22] The 2'-O-methyl (2'-OMe) and 2'-fluorine (2'-F) are widely used modifications, which upon incorporation within oligonucleotides increase the binding affinity toward the complementary strand,[23] thereby increasing their stability.[24] Although both modifications adopt North sugar pucker (3'-endo of the sugar ring),[25] 2'-F modification exhibits stronger gauche effect imparted by the fluorine at the 2' position of the sugar structure. Thereby, 2'-F increases the binding affinity by 2-3 ºC per insert versus DNA, which is due to enthalpy benefits from enhanced base-pairing and stacking interactions arising from the electronegative fluorine.[26] Recently, the use of 2'-OMe modification in the colloid-based detection of short DNA sequences for diagnostic breast cancer[27] has been shown to improve the stability and increase the binding affinity toward the targeted sequence. Thus, chemical modification of the capture probe is a promising strategy to improve the performance of colloidal biosensors.

We have recently reported that the sensitivity of plasmon-assisted SNP detection in ssDNA could be improved by the use of relatively large AuNPs of ~60 nm in diameter.[28] The larger diameter of AuNPs allowed for the reduction of their concentration in the assay, which was critical to maximize the ratio between DNA analyte and AuNPs. To further improve the sensitivity in the detection of SNP in long ssDNA sequences of up to 140 bases,[29] we proposed the so-called preincubation assay. In this system, the capture probes of one Au@DNA batch could disrupt the secondary structure of analyte ssDNA through selective binding. The presence of a second batch Au@DNA caused aggregation and thus improved SNP detection, as compared to the detection without the preincubation. We found recently that purposely designed blocking probes can efficiently block an antisense sequence, thereby preventing reannealing during the cooling step. Although these results represent a step forward the detection of SNP, the complexity of real-world mutations (length and structure of DNA) requires fine-tuning parameters such as the presence of chemically modified DNA capture probes or diameter of the nanoparticles.

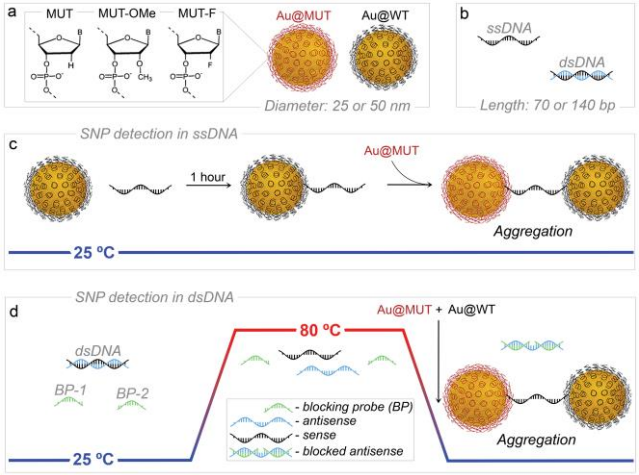

Figure 1. General design of assays and building blocks for discrimination of single nucleotide polymorphism. a) Gold nanoparticles diameter (25 or 50 nm) and chemical modification of capture probes (2'-OMe or 2'-F). b) Target DNA: ssDNA or dsDNA of 70 and 140 bp, carrying SNP mutation. c) Preincubation assay for discrimination of SNP in ssDNA. d) Blocking assay for discrimination of SNP in dsDNA, which requires the use of blocking probes (BP-1 and BP-2) and thermal treatment. The signal readout is achieved by selective nanoparticle aggregation.

We evaluate in this work the role of chemical modifications (2'-OMe and 2'-F) in the colorimetric discrimination of single point mutation in ssDNA and dsDNA (70 and 140 bp) using gold nanoparticles of 25 and 53 nm in diameter (**Fig. 1a,b**). Discrimination of SNP in either ssDNA or dsDNA required different strategies based on the preincubation step (**Fig. 1c**) and blocking strategy combined with thermal annealing (**Fig. 1d**), respectively. Our main finding is that 2'-F modification improves SNP discrimination with ssDNA, while 2'-OMe improved the discrimination with dsDNA. Regardless the modification used, the sensitivity of the assay increased for larger particles while the selectivity was better for smaller particles. For the larger particle diameter, the role of the chemical modification was less pronounced, thus revealing the importance of curvature in the nanoparticles.

METHODS

Chemicals. Hydrogen tetrachloroaurate (III) trihydrate ($HAuCl_4 \cdot 3H_2O$) was purchased from Alfa Aesar. Sodium dodecyl sulfate (SDS) (98%), sodium chloride (NaCl) (99.5%), sodium citrate tribasic dihydrate (98%), and phosphate buffer (PB) 1 M, pH 7.4, were purchased from Sigma-Aldrich. Phosphate buffered saline (PBS) 0.01 M, pH 7.4, containing 0.138 M NaCl and 2.7 mM KCl (Sigma-Aldrich) was used to mimic physiological conditions. DNA targets and thiolated oligonucleotides (see Supporting Information, **Table S1**) were purchased from Biomers (Germany). To quantify the concentration of DNA loaded on NPs, the Quant-iT Oli Green ssDNA Kit from Thermo Fisher Scientific was employed.

Instrumentation. UV–Vis-NIR spectra were measured at room temperature on an Agilent 8453 UV–Vis spectrophotometer, using UV Micro cuvettes with 1 cm optical path length. Transmission electron microscopy (TEM) was measured in a JEOL JEM-1400 PLUS, operating at 120 kV. Dynamic light scattering (DLS) measurements were carried out in a Malvern NanoSizer. Fluorescence measurements were performed in a MicroPlate Reader. A ThermoBath was used for the thermal treatment of the samples.

Synthesis and functionalization of 25 nm and 53 nm AuNPs. AuNPs were synthesized following a seeded growth method.[31] The particles were then functionalized with thiolated oligonucleotides (WT, MUT) according to the method reported by Hurst et al.[32] Briefly, to the AuNPs colloid (1.11 mL) containing SDS (0.1%) and PB (0.01 M) was added a solution of oligonucleotides (0.1 mM). An excess of oligonucleotides was used in all samples. The mixture of oligonucleotides and AuNPs was incubated at room temperature for 20 min. To improve oligonucleotide binding, a salt aging process was carried out. A solution containing NaCl (2 M), SDS (0.01%), and PB (0.01 M) was added sequentially to the mixture containing AuNPs and oligonucleotides, in the following aliquots: 5, 5, 15, 25, and 50 µL, reaching a final NaCl concentration of 0.2 M. Each salt aging step was alternated with sonication (10 s) and incubation (20 min), followed by incubation for 12 h. To remove excess oligonucleotides, the solutions were centrifuged (8500 rpm, 10 min, 3 times) and each time redispersed in SDS (1 mL, 0.01%). The final concentration of nanoparticles was 0.4 mM in terms of Au atoms for all samples.

Quantification of DNA grafted to AuNPs. To determine the number of oligonucleotides per NP, the concentration of NPs was first determined by UV-Vis-NIR spectroscopy.[33] Then, the oligonucleotides were detached from the NPs surface using dithiothreitol in equal volumes. After incubation (1 hour) the precipitate was discarded by centrifugation. The supernatant (25 µL) was added to Tris-EDTA buffer (75 µL), followed by addition of OliGreen

reagent (100 µL) and incubation for 5 minutes at room temperature, protected from light. Fluorescence was measured and compared to a standard curve. For fluorescence measurements, the fluorophore was excited at 485 nm and the emission was recorded at 535 nm. The amount of DNA per NP was calculated dividing the concentration of oligonucleotides by the concentration of NPs.

Detection of ssDNA – Preincubation assay. To the solution containing Au@WT (62.5 µL) and PBS (x1, 325 µL) was added a mixture (50 µL) containing PB (0.01 M) and NaCl (2 M). Subsequently, an aliquot of target ssDNA (either match or mismatch) was added to the solution and incubated in a roller mixer. After 1 hour, Au@MUT or the corresponding modifications (62.5 µL) were added and the incubation process continued for 4 hours. UV-Vis-NIR spectra were recorded every hour.

Detection of dsDNA – Blocking assay. In an Eppendorf tube, PBS (x1, 325 µL) was added to 50 µL of a mixture containing PB (0.01 M) and NaCl (2 M). Equal volumes of blocking probe 1 (BP-1) and blocking probe 2 (BP-2) (2.5 µL) were added to the solution, reaching a concentration of 5 nM. Finally, an aliquot of 70 or 140 bases target dsDNA (either match or mismatch) at a concentration of 5 nM was added to the solution. The temperature of the mixture was then increased from 25 ºC to 80 ºC in a ThermoBath and maintained for 10 min. The mixture was removed from the ThermoBath and cooled down to room temperature (3ºC / min). This solution was added into a UV Mikro cuvette containing equal volumes (62.5 µL) of two batches of NPs (Au@WT and Au@MUT or the corresponding modifications). UV-Vis-NIR measurements were performed every hour.

Dynamic Light Scattering. The conditions for DLS experiments were: 6 measurements with 5 runs of 5 s each. The study was carried out at 25 ºC with an equilibration time of the sample of 30 s.

The simulations of binding affinities for blocking probes were performed using UNAFold software (http://unafold.rna.albany.edu/?q=DINAMelt/software)

RESULTS AND DISCUSSION

Our assays involved two batches of AuNPs (25.4 ± 0.3 or 53.1 ± 0.4 nm) stabilized with DNA (capture probes), complementary either to the unaltered part of the target DNA (Au@WT) or to the segment carrying mutation (Au@MUT) (**Table S1**). The chemical modification of the MUT capture probes were introduced at the 2' position of the sugar ring substituting thus the hydrogen atom by either O-Me (Au@MUT-OMe) or by fluorine (Au@MUT-F) (**Fig. 1a**). Only three bases of the MUT sequence were chemically modified and were located in the region corresponding to SNP of target sequence (**Table S1**). Our model target carried an L858R mutation, which occurs in the Epidermal Growth Factor Receptor (*EGFR*) gene. This mutation is present in 10-20% patents with non-small cell lung cancer.[34] To mimic a real-world scenario, we used targets of 70 and 140 bp in length, in the form of both single and double-stranded DNA (**Fig. 1b**).

Since the detection of SNP in single or double-stranded DNA requires different mechanisms, we implemented two assays. On one hand, we used our recently reported *preincubation* assay[29] for SNP discrimination in ssDNA, and on the other hand a novel *blocking* assay for dsDNA. The preincubation assay comprised two steps: (1) preincubation of the ssDNA target with Au@WT for 1 hour and (2) addition of Au@MUT to induce gradual aggregation (**Fig. 1c**). The blocking assay, on the other hand, comprised three steps: (1) combination of two types of blocking probes, BP-1 (11 bases) and BP-2 (12 bases), as well as the analyte dsDNA; (2) thermal treatment of the mixture for 10 min at 80 ºC followed by cooling down to room temperature for 20 min; (3) addition of Au@WT and Au@MUT (**Fig. 1d**). The performance of both assays was evaluated optically by defining the unitless magnitude R = Abs_{640}/Abs_{max}, as a measure of the degree of aggregation.[35]

The complementarity between the blocking probes and the antisense sequence of analyte dsDNA caused non-specific aggregation of nanoparticles in the presence of BPs (BP-1 is complementary to Au@MUT, while BP-2 is complementary to Au@WT). Maeda and co-workers[36,37] have shown that non-specific aggregation occurs upon the transition from ssDNA to dsDNA and is conditioned by the alteration of the initial balance between steric repulsion and van der Waals attraction. To determine a limiting concentration of BPs in our blocking assay, we evaluated the stability of the nanoparticles within a wide concentration range of BPs. We found that increasing BP concentration from 1 to 100 nM leads to a gradual increase in non-specific aggregation (**Fig. 2a**). Plotting R@10min *vs.* [BP] revealed an inflection point of the aggregation rate at [BP] = 20 nM. Considering that each particle is coated by ~1500 capture probes (see experimental part) and that the total concentration of capture probe in the solution is 19.5 nM, we assume that the inflection point at 20 nM [BP] corresponds to full coverage of the NPs with BPs. Importantly, AuNPs remain stable below 5 nM of BPs (**Fig. 2b – grey area**), which we set as the upper concentration limit in the subsequent studies. We also evaluated the stability of AuNPs carrying DNA with 2'-OMe and 2'-F modifications, in the presence of blocking probes (5 nM), showing that both chemical modifications improve the colloidal stability of the nanoparticles for longer periods of time (**Fig. 2b inset**).

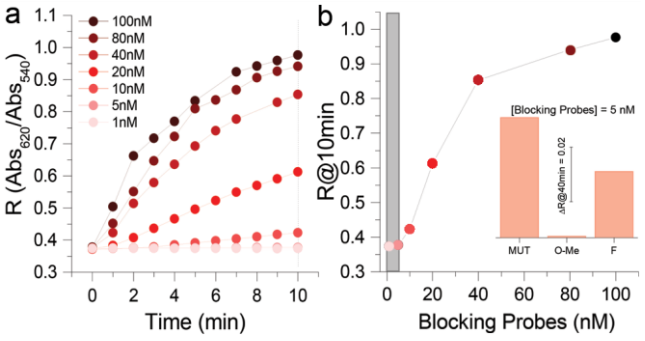

Fig. 2. Allowed concentration range of blocking probes. a) aggregation rate of AuNPs at different concentrations of blocking sequences. b) Aggregation degree at 10 min, showing the limit of [BP] concentration < 5 nM (grey band), below which particles remain stable. Inset: colloidal stability of

AuNPs stabilized with chemically modified capture probes after 40 min. in the presence of [BP] = 5 nM.

To further understand the efficiency of each blocking probe, we monitored the performance of the blocking assay (Au@MUT-OMe, Au@WT, 53 nm) using dsDNA (70 and 140 bp) and the following blocking combinations: (1) BP-1 + BP-2; (2) BP-2; (3) BP-1; (4) no BP (see **Fig. 3**). The presence of two blocking probes was found to lead to a better signal detection – higher blocking power of the antisense strand – as compared to the use of BP-1 or BP-2 alone, which is in agreement with our previous observations.[30] The superior performance of the assay involving two blocking probes is related to these small sequences hindering the renaturation of the complementary strands (sense and antisense). This renaturation process starts with the hybridization of the oligonucleotides located in the middle of the strands[38] once the temperature drops below T_m. The blocked antisense sequence cannot rehybridize with the sense sequence, which can then be captured by the AuNPs. Time-dependent DLS measurements showed pronounced clustering for both blocking probes as compared to smaller clusters in a solution without BP (**Fig. S2**).

Interestingly, BP-2 exhibits better blocking performance than BP-1, which is attributed to the high GC content in BP1 (72%), as compared to only 42% in BP-2. Also, the longer BP-2 (12 nucleotides) as compared to BP-1 (10 nucleotides) suggests higher melting temperature for an antisense-BP-2 couple. Thus, the blocking events by BP-2 take place earlier during the cooling process. This statement is further supported by simulated values of the free energy of hybridization (25 ºC and [NaCl]=0.3 M). The transition from a BP2-Au@WT couple to a BP2-antisense couple is more favorable (ΔG = -3.9 kcal/mol) than the transition from BP1-Au@MUT to a BP1-antisense couple (ΔG = 0 kcal/mol). It is also worth mentioning that the trend of the aggregation degree for the different blocking scenarios was maintained for longer dsDNA (140 bp), but the R values were lower, confirming again that the length of the target decreases the sensitivity of the assay (**Fig. 3b**).

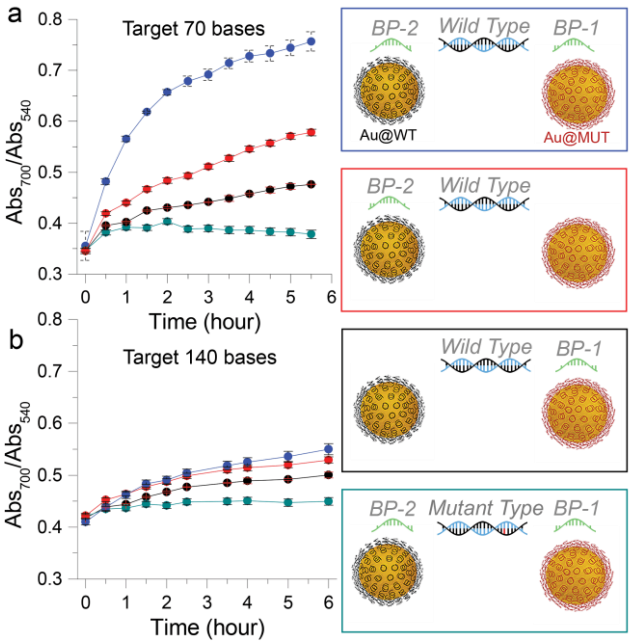

Fig. 3. Optimization of blocking probes efficiency. a, b) Aggregation rates for different blocking strategies: BP-1 and BP2 (blue, green), BP-2 (red), BP-1 (black) for dsDNA match (blue, red, black) and mismatch (green) analyte of 70 bases (a) and 140 bases (b). In both cases, blocking probes and target concentrations were kept constant (5 nM).

Next, we evaluated the capacity of the blocking assay toward discriminating the presence of a single point mutation, observing suppressed aggregation of AuNPs in the case of mutation (**Fig. 3** – blue vs. green). These data confirm that the blocking assay can indeed discriminate mutations in long sequences of clinical relevance, in a one-pot process that can even be detected by the naked-eye (**Fig. S1**), in agreement with DLS measurements (**Fig. S2).** The dynamic range of the sensors for match sequence detection was estimated to be in the range of 5 fmol to 20 pmol (**Fig. S3**).

Although the thermal treatment step was mandatory to induce selective aggregation in the blocking assay (**Fig. S4**), the thermal treatment without blocking probes caused a slight aggregation, in the presence of both match and mismatch sequences (70 or 140 bases) (**Fig. S5**). Aggregation of AuNPs in the absence of BP is likely to occur because the capture probes themselves can play the role of blocking probes. A four-fold concentration of capture probes in solution, as compared to blocking probes, can prevent the formation of sense-antisense dimers upon cooling.

To obtain a more detailed picture of the way chemical modification affects the selectivity and sensitivity of both assays, we performed a set of 48 experiments (**Fig. S6-S8**), in which we combined the following parameters: length (70 or 140 bp), structure of target (ssDNA or dsDNA), size of AuNPs (25 or 53 nm) and type of chemical modification (2'-OMe, 2'-F). The first observation was that the sensitivity and selectivity decreased when increasing the length of the DNA analyte (**Fig. S7**). For the sake of clarity, the whole dataset was simplified by averaging R values for

both 70 and 140 bp, thereby facilitating the comparison between chemical modifications (for individual analysis see **Figs. S10&11**). **Fig. 4a b** displays aggregation values for perfect match (sensitivity), while **Fig. 4c, d** shows the difference in aggregation degree for the match and the mismatch (selectivity), for both ssDNA and dsDNA. These analyses confirmed that on average the sensitivity of ssDNA detection is higher than that of dsDNA, which is due to the chemical crowdedness in the blocking assay containing antisense strands and blocking probes.

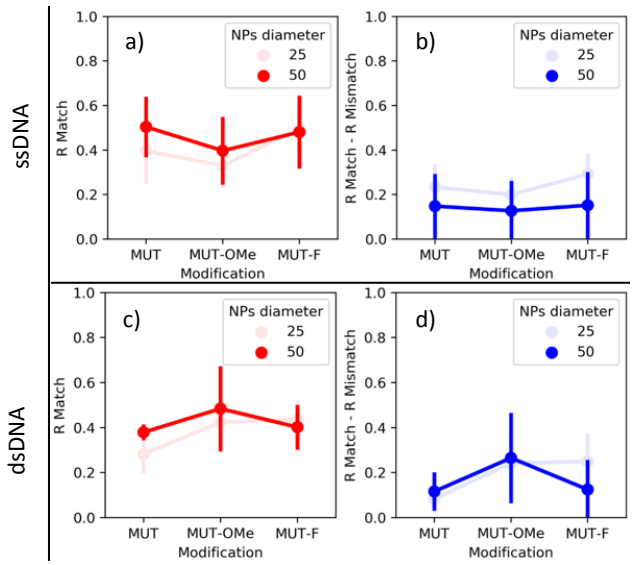

Fig. 4. The effect of chemical modifications on sensitivity (aggregation degree for match sequence) (a,c) and selectivity (aggregation degree difference for match and mismatch sequences) (b, d) for the preincubation assay (a, b) and the blocking assay (c,d).

The 2'-F modification improves the sensitivity of ssDNA detection, that is especially visible for smaller nanoparticles (**Fig. 4a**). Such trend can be explained by the higher binding affinity of fluorine-based modification as compared to 2'-OMe that is also confirmed by the faster aggregation rate of nanoparticles carrying 2'-F modifications (**Fig. S9**). On the contrary, the sensitivity of dsDNA (blocking assay) is more pronounced for 2'-OMe modification as compared aggregation in the presence of fluorine (**Fig. 4c**). This is presumably because the superior affinity of 2'-F leads to the undesired interactions of nanoparticles with the blocking probes and antisense sequences. Therefore, bulky 2'-OMe modification is convenient modification for detection of dsDNA while 2'-F modification performs better for ssDNA where no interfering sequences are present.

Smaller nanoparticles showed a better selectivity towards a single base variation, as compared to the large particles (**Fig 4b**). The surface curvature may induce changes in the cooperative effect during the hybridization of complementary DNA strands, thus leading to less selective discrimination of SNP when increasing AuNP diameter. The effect of DNA modifications on the selectivity of the assays follows the same trend as for the sensitivity. In ssDNA detection, the largest difference between the aggregation degrees of the match and the mismatch sequences was achieved with 2'-F modifications. In the case of the dsDNA detection, 2'-OMe modification showed the best performance.

CONCLUSIONS

We report the effect of chemical modifications (2'-OMe and 2'-F) incorporated in DNA-stabilized AuNPs for the discrimination of single-nucleotide polymorphism in ssDNA and dsDNA, of clinically relevant lengths (70 and 140 bp). We implemented different assays, namely a preincubation assay for SNP detection in ssDNA, and a blocking assay for dsDNA. We observed that higher binding affinity and small size of 2'-F modification in capture probes leads to better discrimination of SNP in single-stranded DNA. On the other hand, bulky 2'-OMe modification improves the discrimination of SNP in dsDNA where the antisense and blocking probes increase the chemical crowdedness. Overall, our findings indicate that the chemical complexity of a biomolecular environment requires careful design of colloid-based biosensors, where particle size and chemical modification define the final performance of the assay.

ASSOCIATED CONTENT

Supporting Information. DNA sequences, dynamic range, DLS measurements, control experiments without blocking probes and thermal treatment, aggregation degree for the mismatch sequence. This material is available free of charge via the Internet at http://pubs.acs.org.

AUTHOR INFORMATION

Corresponding Author

* Email: marek.grzelczak@dipc.org

Notes

The authors declare no competing financial interest.

ACKNOWLEDGMENT

This work was supported by the Spanish Ministerio de Economia y Competitividad MINECO (grants: MAT2013-46101-R, MAT2013-49375-EXP, MAT2017-86659-R) and FEDER funds (PI12/00663, PIE13/00048, DTS14/00109, PI15/00275).

REFERENCES

(1) Smith, S. J.; Nemr, C. R.; Kelley, S. O. Chemistry-Driven Approaches for Ultrasensitive Nucleic Acid Detection. J. Am. Chem. Soc. 2017, 139 (3), 1020–1028.

(2) Chan, K. C. A.; Jiang, P.; Zheng, Y. W. L.; Liao, G. J. W.; Sun, H.; Wong, J.; Siu, S. S. N.; Chan, W. C.; Chan, S. L.; Chan, A. T. C.; et al. Cancer Genome Scanning in Plasma: Detection of Tumor-Associated Copy Number Aberrations, Single-Nucleotide Variants, and Tumoral Heterogeneity by Massively Parallel Sequencing. Clin. Chem. 2013, 59 (1), 211–224.

(3) Yung, T. K. F.; Chan, K. C. A.; Mok, T. S. K.; Tong, J.; To, K.-F.; Lo, Y. M. D. Single-Molecule Detection of Epidermal Growth Factor Receptor Mutations in Plasma by Microfluidics Digital PCR in Non-Small Cell Lung Cancer Patients. Clin. Cancer Res. Off. J. Am. Assoc. Cancer Res. 2009, 15 (6), 2076–2084.

(4) Diehl, F.; Li, M.; Dressman, D.; He, Y.; Shen, D.; Szabo, S.; Diaz, L. A.; Goodman, S. N.; David, K. A.; Juhl, H.; et al. Detection

and Quantification of Mutations in the Plasma of Patients with Colorectal Tumors. Proc. Natl. Acad. Sci. U. S. A. 2005, 102 (45), 16368–16373.

(5) Qiu, M.; Wang, J.; Xu, Y.; Ding, X.; Li, M.; Jiang, F.; Xu, L.; Yin, R. Circulating Tumor DNA Is Effective for the Detection of EGFR Mutation in Non–Small Cell Lung Cancer: A Meta-Analysis. Cancer Epidemiol. Prev. Biomark. 2015, 24 (1), 206–212.

(6) Freidin, M. B.; Freydina, D. V.; Leung, M.; Fernandez, A. M.; Nicholson, A. G.; Lim, E. Circulating Tumor DNA Outperforms Circulating Tumor Cells for KRAS Mutation Detection in Thoracic Malignancies. Clin. Chem. 2015, 61 (10), 1299–1304.

(7) Chan, K. C. A.; Jiang, P.; Chan, C. W. M.; Sun, K.; Wong, J.; Hui, E. P.; Chan, S. L.; Chan, W. C.; Hui, D. S. C.; Ng, S. S. M.; et al. Noninvasive Detection of Cancer-Associated Genome-Wide Hypomethylation and Copy Number Aberrations by Plasma DNA Bisulfite Sequencing. Proc. Natl. Acad. Sci. 2013, 110 (47), 18761–18768.

(8) Balgkouranidou, I.; Chimonidou, M.; Milaki, G.; Tsarouxa, E. G.; Kakolyris, S.; Welch, D. R.; Georgoulias, V.; Lianidou, E. S. Breast Cancer Metastasis Suppressor-1 Promoter Methylation in Cell-Free DNA Provides Prognostic Information in Non-Small Cell Lung Cancer. Br. J. Cancer 2014, 110 (8), 2054–2062.

(9) Wang, X.; Lim, H. J.; Son, A. Characterization of Denaturation and Renaturation of DNA for DNA Hybridization. Environ. Health Toxicol. 2014, 29.

(10) Draz, M. S.; Shafiee, H. Applications of Gold Nanoparticles in Virus Detection. Theranostics 2018, 8 (7), 1985–2017.

(11) Grzelczak, M.; Pérez-Juste, J.; Mulvaney, P.; Liz-Marzán, L. M. Shape Control in Gold Nanoparticle Synthesis. Chem. Soc. Rev. 2008, 37 (9), 1783–1791.

(12) Nath, N.; Chilkoti, A. A Colorimetric Gold Nanoparticle Sensor To Interrogate Biomolecular Interactions in Real Time on a Surface. Anal. Chem. 2002, 74 (3), 504–509.

(13) Xue, C.; Li, Z.; Mirkin, C. A. Large-Scale Assembly of Single-Crystal Silver Nanoprism Monolayers. Small 2005, 1 (5), 513–516.

(14) Kelley, S. O.; Mirkin, C. A.; Walt, D. R.; Ismagilov, R. F.; Toner, M.; Sargent, E. H. Advancing the Speed, Sensitivity and Accuracy of Biomolecular Detection Using Multi-Length-Scale Engineering. Nat. Nanotechnol. 2014, 9 (12), 969–980.

(15) Das, J.; Ivanov, I.; Montermini, L.; Rak, J.; Sargent, E. H.; Kelley, S. O. An Electrochemical Clamp Assay for Direct, Rapid Analysis of Circulating Nucleic Acids in Serum. Nat. Chem. 2015, 7 (7), 569–575.

(16) Das, J.; Ivanov, I.; Sargent, E. H.; Kelley, S. O. DNA Clutch Probes for Circulating Tumor DNA Analysis. J. Am. Chem. Soc. 2016, 138 (34), 11009–11016.

(17) Yang, B.; Gu, K.; Sun, X.; Huang, H.; Ding, Y.; Wang, F.; Zhou, G.; Huang, L. L. Simultaneous Detection of Attomolar Pathogen DNAs by Bio-MassCode Mass Spectrometry. Chem. Commun. 2009, 46 (43), 8288–8290.

(18) Mulvaney, S. P.; Ibe, C. N.; Tamanaha, C. R.; Whitman, L. J. Direct Detection of Genomic DNA with Fluidic Force Discrimination Assays. Anal. Biochem. 2009, 392 (2), 139–144.

(19) Klamp, T.; Camps, M.; Nieto, B.; Guasch, F.; Ranasinghe, R. T.; Wiedemann, J.; Petrášek, Z.; Schwille, P.; Klenerman, D.; Sauer, M. Highly Rapid Amplification-Free and Quantitative DNA Imaging Assay. Sci. Rep. 2013, 3, 1852.

(20) Massey, M.; Krull, U. J. A Fluorescent Molecular Switch for Room Temperature Operation Based on Oligonucleotide Hybridization without Labeling of Probes or Targets. Anal. Chim. Acta 2012, 750 (Supplement C), 182–190.

(21) Hill, H. D.; Vega, R. A.; Mirkin, C. A. Non-Enzymatic Detection of Bacterial Genomic DNA Using the Bio-Barcode Assay. Anal. Chem. 2007, 79 (23), 9218–9223.

(22) Kurreck, J. Antisense Technologies. Eur. J. Biochem. 2003, 270 (8), 1628–1644.

(23) Majlessi, M.; Nelson, N. C.; Becker, M. M. Advantages of 2′-O-Methyl Oligoribonucleotide Probes for Detecting RNA Targets. Nucleic Acids Res. 1998, 26 (9), 2224–2229.

(24) Rettig, G. R.; Behlke, M. A. Progress toward in Vivo Use of siRNAs-II. Mol. Ther. J. Am. Soc. Gene Ther. 2012, 20 (3), 483–512.

(25) Ikeda, H.; Fernandez, R.; Wilk, A.; Barchi, J. J.; Huang, X.; Marquez, V. E. The Effect of Two Antipodal Fluorine-Induced Sugar Puckers on the Conformation and Stability of the Dickerson-Drew Dodecamer Duplex [d(CGCGAATTCGCG)]2. Nucleic Acids Res. 1998, 26 (9), 2237–2244.

(26) Pallan, P. S.; Greene, E. M.; Jicman, P. A.; Pandey, R. K.; Manoharan, M.; Rozners, E.; Egli, M. Unexpected Origins of the Enhanced Pairing Affinity of 2′-fluoro-Modified RNA. Nucleic Acids Res. 2011, 39 (8), 3482–3495.

(27) Li, J.; Huang, J.; Yang, X.; Yang, Y.; Quan, K.; Xie, N.; Wu, Y.; Ma, C.; Wang, K. Gold Nanoparticle-Based 2′-O-Methyl Modified DNA Probes for Breast Cancerous Theranostics. Talanta 2018, 183, 11–17.

(28) Sanromán-Iglesias, M.; Lawrie, C. H.; Schäfer, T.; Grzelczak, M.; Liz-Marzán, L. M. Sensitivity Limit of Nanoparticle Biosensors in the Discrimination of Single Nucleotide Polymorphism. ACS Sens. 2016, 1 (9), 1110–1116.

(29) Sanromán-Iglesias, M.; Lawrie, C. H.; Liz-Marzán, L. M.; Grzelczak, M. Nanoparticle-Based Discrimination of Single-Nucleotide Polymorphism in Long DNA Sequences. Bioconjug. Chem. 2017, 28 (4), 903–906.

(30) Aboudzadeh, M. A.; Sanromán-Iglesias, M.; Lawrie, C. H.; Grzelczak, M.; Liz-Marzán, L. M.; Schäfer, T. Blocking Probe as a Potential Tool for Detection of Single Nucleotide DNA Mutations: Design and Performance. Nanoscale 2017, 9 (42), 16205–16213.

(31) Bastús, N. G.; Comenge, J.; Puntes, V. Kinetically Controlled Seeded Growth Synthesis of Citrate-Stabilized Gold Nanoparticles of up to 200 Nm: Size Focusing versus Ostwald Ripening. Langmuir 2011, 27 (17), 11098–11105.

(32) Hurst, S. J.; Lytton-Jean, A. K. R.; Mirkin, C. A. Maximizing DNA Loading on a Range of Gold Nanoparticle Sizes. Anal. Chem. 2006, 78 (24), 8313–8318.

(33) Scarabelli, L.; Grzelczak, M.; Liz-Marzán, L. M. Tuning Gold Nanorod Synthesis through Prereduction with Salicylic Acid. Chem. Mater. 2013, 25 (21), 4232–4238.

(34) Sharma, S. V.; Bell, D. W.; Settleman, J.; Haber, D. A. Epidermal Growth Factor Receptor Mutations in Lung Cancer. Nat. Rev. Cancer 2007, 7 (3), 169–181.

(35) Liu, Y.; Liu, Y.; Mernaugh, R. L.; Zeng, X. Single Chain Fragment Variable Recombinant Antibody Functionalized Gold Nanoparticles for a Highly Sensitive Colorimetric Immunoassay. Biosens. Bioelectron. 2009, 24 (9), 2853–2857.

(36) Akiyama, Y.; Shikagawa, H.; Kanayama, N.; Takarada, T.; Maeda, M. DNA Dangling-End-Induced Colloidal Stabilization of Gold Nanoparticles for Colorimetric Single-Nucleotide Polymorphism Genotyping. Chem. – Eur. J. 2014, 20 (52), 17420–17425.

(37) Sato, K.; Hosokawa, K.; Maeda, M. Rapid Aggregation of Gold Nanoparticles Induced by Non-Cross-Linking DNA Hybridization. J. Am. Chem. Soc. 2003, 125 (27), 8102–8103.

(38) Sedighi, A.; Li, P. C. H.; Pekcevik, I. C.; Gates, B. D. A Proposed Mechanism of the Influence of Gold Nanoparticles on DNA Hybridization. ACS Nano 2014, 8 (7), 6765–6777.

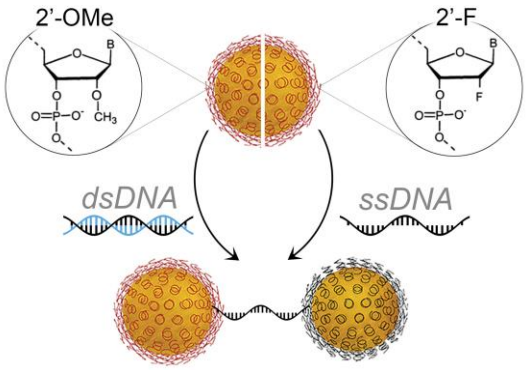

Chemical modifications improve the performance of colorimetric biosensors in the discrimination of single point mutation in clinically-relevant DNA targets.